TABLE 3. Numbers of clinically definite infections and CMV antigenemia among the three regimens

	RIST with ATG (n=20)	RIST without ATG (n=19)	CST (n=33)	P value
Infection	11	11	20	0.94
Bacteria				
Bacteremia	9	8	12	0.98
Pneumonia	1	3	4	
Anal abscess	1	—	—	
Spleen abscess	—	—	1	
Pyelonephritis	—	—	1	
Fungus				
Aspergillus	—	2	2	
Virus				
CMV	—	—	4	
VZV	1	—	—	
Adeno	—	1	6	
PCP	1	—	—	
CMV antigenemia	9	10	21	0.50
Rising antigenemia	3	7	4	0.08

VZV, varicella zoster virus; PCP, *Pneumocystis carinii* pneumonia.

over, the median number of days to the onset of acute GVHD was 17, which was shorter than in our analysis. However, it is not possible to directly compare their results with either our present findings or those of Slavin and coworkers because they used methotrexate or mycophenolate mofetil in addition to CsA as prophylaxis against GVHD, whereas we did not. Likewise, additional intensive immunosuppression with CAMPATH-1H resulted in the reduction of acute and chronic GVHD (*26*). Furthermore, we still have to consider the possibility that the difference in the patients' background, including the disease status and pretransplantation treatment history, affected the occurrence of acute GVHD, although this was discounted by the results of a multivariate analysis.

An additional important finding in this study is the close chronologic relationship between the onset of acute GVHD and the induction of mixed T-cell chimerism in RIST. Whenever GVHD occurred, the onset was significantly delayed in RIST without ATG compared with the conventional regimen, despite the fact that the overall incidence of acute GVHD in RIST without ATG was high compared with that in CST. Other recent reports have noted that the achievement of T cell complete chimera preceded the onset of acute GVHD (*4,27*) (i.e., the incidence of GVHD might become low under mixed T-cell chimerism, although controversial data have been published; 28). In any event, the results suggest that the delayed achievement of donor T-cell chimerism may contribute to the delayed onset of acute GVHD.

There is a concern that the use of ATG may increase the rate of serious infections, including CMV infection (*29*). However, in the present study, our analysis of risk factors for CMV infection, especially rising antigenemia, showed that both acute GVHD and steroid therapy were significant factors, whereas ATG was not. Moreover, the observed incidence of clinically definitive infection, which included CMV, was comparable among the three regimens. It is likely that the higher risk of CMV infection with the use of ATG more than offsets the risk of more frequent use of steroids to control the higher incidence of GVHD in those who were not treated with ATG.

In our immunophenotype analysis, the reconstitution of $CD3^+/CD4^+$ cells could be clearly divided into three characteristic patterns. The number of $CD4^+/CD45^+RA$ cells (naive $CD4^+$ T cell) in RIST with ATG remained significantly lower than in the other two regimens. Because ATG has a prolonged half-life in humans (*30*), the combination of CsA and ATG could intensively deplete T lymphocytes in donor PBSC graft to suppress the regeneration of T lymphopoiesis after engraftment (*31*). Therefore, it is likely that this delayed reconstitution of naive $CD4^+$ T cells resulted in the lower incidence of GVHD in RIST with ATG, because interaction between naive $CD4^+$ T cells and DC is critical for mediating the immune response (*32*). DC2 induce naive $CD4^+$ T cells toward Th2 cells, which secrete immunosuppressive cytokines, IL-4 and IL-10, to suppress GVHD. Hence, the kinetics of naive $CD4^+$ T cells may play a crucial role in the development of GVHD. In our study, the DC1/DC2 ratio was greater than 1.0 after day 30, with no difference among the three regimens. Because the function of DC1 seemed to be the same in the three cohorts, the low number of naive $CD4^+$ T cells may have partly contributed to the development of GVHD.

CONCLUSION

We examined the effect of adding ATG to a RIST conditioning regimen. We found that the development kinetics of acute and chronic GVHD after RIST are complex, because they are sensitively modulated by the use of immunosuppressive therapy before and after transplantation and the variable use of steroids. Nonetheless, our results suggest that naive $CD4^+$ T cells may affect the development of GVHD and that the delayed achievement of complete T-cell chimerism in a regimen without ATG may be responsible for the delayed onset of acute GVHD. The control of GVHD with ATG may still outweigh the suggested risk of infections, which is increased with the use of steroid. Considering these findings together, the conditioning regimen and immunosuppressive strategy should be carefully designed after RIST and should depend on the urgent risk of disease recurrence and GVHD.

REFERENCES

1. Thomas ED, Storb R, Clift RA, et al. Bone-marrow transplantation (second of two parts). N Engl J Med 1975; 292: 895.
2. Slavin S, Nagler A, Naparstek E, et al. Nonmyeloablative stem cell transplantation and cell therapy as an alternative to conventional bone marrow transplantation with lethal cytoreduction for the treatment of malignant and nonmalignant hematologic diseases. Blood 1998; 91: 756.
3. Horowitz MM, Gale RP, Sondel PM, et al. Graft-versus-leukemia reactions after bone marrow transplantation. Blood 1990; 75: 555.
4. McSweeney PA, Niederwieser D, Shizuru JA, et al. Hematopoietic cell transplantation in older patients with hematologic malignancies: replacing high-dose cytotoxic therapy with graft-versus-tumor effects. Blood 2001; 97: 3390.
5. Szczech LA, Berlin JA, Feldman HI. The effect of antilymphocyte induction therapy on renal allograft survival: a meta-analysis of individual patient-level data. Ann Intern Med 1998; 128: 817.
6. Saito T, Kanda Y, Kami M, et al. Therapeutic potential of a reduced-intensity preparative regimen for allogeneic transplantation with cladribine, busulfan, and antithymocyte globulin against advanced/refractory acute leukemia/lymphoma. Clin Cancer Res 2002; 8: 1014.
7. Niiya Y, Kanda Y, Saito T, et al. Early full donor myeloid chimerism after reduced-intensity stem cell transplantation using a combination of fludarabine and busulfan. Haematologica 2001; 86: 1071.
8. Lazarus HM, Vogelsang GB, Rowe JM. Prevention and treatment of acute

graft-versus-host disease: the old and the new. A report from the Eastern Cooperative Oncology Group (ECOG). Bone Marrow Transplant 1997; 19: 577.
9. Liu YJ. Dendritic cell subsets and lineages, and their functions in innate and adaptive immunity. Cell 2001; 106: 259.
10. Banchereau J, Steinman RM. Dendritic cells and the control of immunity. Nature 1998; 392: 245.
11. O'Doherty U, Peng M, Gezelter S, et al. Human blood contains two subsets of dendritic cells, one immunologically mature and the other immature. Immunology 1994; 82: 487.
12. Rissoan MC, Soumelis V, Kadowaki N, et al. Reciprocal control of T helper cell and dendritic cell differentiation. Science 1999; 283: 1183.
13. Abbas AK, Murphy KM, Sher A. Functional diversity of helper T lymphocytes. Nature 1996; 383: 787.
14. Breathnach SM, Katz SI. Effect of X-irradiation on epidermal immune function: decreased density and alloantigen-presenting capacity of Ia+ Langerhans cells and impaired production of epidermal cell-derived thymocyte activating factor (ETAF). J Invest Dermatol 1985; 85: 553.
15. Zambruno G, Girolomoni G, Manca V, et al. Epidermal Langerhans cells after allogeneic bone marrow transplantation: depletion by chemotherapy conditioning regimen alone. J Cutan Pathol 1992; 19: 187.
16. Auffermann-Gretzinger S, Lossos IS, Vayntrub TA, et al. Rapid establishment of dendritic cell chimerism in allogeneic hematopoietic cell transplant recipients. Blood 2002; 99: 1442.
17. Morishima Y, Morishita Y, Tanimoto M, et al. Low incidence of acute graft-versus-host disease by the administration of methotrexate and cyclosporine in Japanese leukemia patients after bone marrow transplantation from human leukocyte antigen compatible siblings: possible role of genetic homogeneity. The Nagoya Bone Marrow Transplantation Group. Blood 1989; 74: 2252.
18. Przepiorka D, Weisdorf D, Martin P, et al. 1994 Consensus Conference on Acute GVHD Grading. Bone Marrow Transplant 1995; 15: 825.
19. Atkinson K, Horowitz MM, Gale RP, et al. Consensus among bone marrow transplanters for diagnosis, grading and treatment of chronic graft-versus-host disease. Committee of the International Bone Marrow Transplant Registry. Bone Marrow Transplant 1989; 4: 247.
20. Kanda Y, Mineishi S, Saito T, et al. Pre-emptive therapy against cytomegalovirus (CMV) disease guided by CMV antigenemia assay after allogeneic hematopoietic stem cell transplantation: a single-center experience in Japan. Bone Marrow Transplant 2001; 27: 437.
21. Nichols WG, Corey L, Gooley T, et al. Rising pp65 antigenemia during preemptive anticytomegalovirus therapy after allogeneic hematopoietic stem cell transplantation: risk factors, correlation with DNA load, and outcomes. Blood 2001; 97: 867.
22. Willmann K, Dunne JF. A flow cytometric immune function assay for human peripheral blood dendritic cells. J Leukocyte Biol 2000; 67: 536.
23. Bacigalupo A, Lamparelli T, Bruzzi P, et al. Antithymocyte globulin for graft-versus-host disease prophylaxis in transplants from unrelated donors: 2 randomized studies from Gruppo Italiano Trapianti Midollo Osseo (GITMO). Blood 2001; 98: 2942.
24. Storb R, Deeg HJ, Pepe M, et al. Methotrexate and cyclosporine versus cyclosporine alone for prophylaxis of graft-versus-host disease in patients given HLA-identical marrow grafts for leukemia: long-term follow-up of a controlled trial. Blood 1989; 73: 1729.
25. Bornhauser M, Thiede C, Schuler U, et al. Dose-reduced conditioning for allogeneic blood stem cell transplantation: durable engraftment without antithymocyte globulin. Bone Marrow Transplant 2000; 26: 119.
26. Kottaridis PD, Milligan DW, Chopra R, et al. In vivo CAMPATH-1H prevents graft-versus-host disease following nonmyeloablative stem cell transplantation. Blood 2000; 96: 2419.
27. Childs R, Clave E, Contentin N, et al. Engraftment kinetics after nonmyeloablative allogeneic peripheral blood stem cell transplantation: full donor T-cell chimerism precedes alloimmune responses. Blood 1999; 94: 3234.
28. Mattsson J, Uzunel M, Brune M, et al. Mixed chimaerism is common at the time of acute graft-versus-host disease and disease response in patients receiving non-myeloablative conditioning and allogeneic stem cell transplantation. Br J Haematol 2001; 115: 935.
29. Kanda Y, Mineishi S, Nakai K, et al. Frequent detection of rising cytomegalovirus antigenemia after allogeneic stem cell transplantation following a regimen containing antithymocyte globulin. Blood 2001; 97: 3676.
30. Bunn D, Lea CK, Bevan DJ, et al. The pharmacokinetics of anti-thymocyte globulin (ATG) following intravenous infusion in man. Clin Nephrol 1996; 45: 29.
31. Muller TF, Grebe SO, Neumann MC, et al. Persistent long-term changes in lymphocyte subsets induced by polyclonal antibodies. Transplantation 1997; 64: 1432.
32. Lanzavecchia A, Sallusto F. Regulation of T cell immunity by dendritic cells. Cell 2001; 106: 263.

Revision of the International Neuroblastoma Pathology Classification

Confirmation of Favorable and Unfavorable Prognostic Subsets in Ganglioneuroblastoma, Nodular

Michel Peuchmaur, M.D.[1]
Emanuele S. G. d'Amore, M.D.[2]
Vijay V. Joshi, M.D.[3]
Jun-ichi Hata, M.D.[4]
Borghild Roald, M.D.[5]
Louis P. Dehner, M.D.[6]
Robert B. Gerbing, M.A.[7]
Daniel O. Stram, Ph.D.[7]
John N. Lukens, M.D.[8]
Katherine K. Matthay, M.D.[9]
Hiroyuki Shimada, M.D., Ph.D.[10]

[1] Service de Pathologie, Hôpital Robert Debré, Paris, France.

[2] Servizio di Anatomia Pathologica, Ospedale S. Bortolo, Vicenza, Italy.

[3] Department of Pathology and Laboratory Medicine, Hartford Hospital, Hartford, Connecticut.

[4] National Research Institute for Child Health and Development, Tokyo, Japan.

[5] Faculty of Medicine, University of Oslo, Oslo, Norway.

[6] Division of Anatomic Pathology, Washington University School of Medicine, St. Louis, Missouri.

[7] The Children's Oncology Group Operations Center, Arcadia, California.

[8] Pediatric Hematology/Oncology, Vanderbilt University Medical Center, Nashville, Tennessee.

[9] Pediatric Hematology/Oncology, University of San Francisco, San Francisco, California.

[10] Department of Pathology and Laboratory Medicine, Childrens Hospital Los Angeles, Los Angeles, California.

This part of the activity of the International Neuroblastoma Pathology Committee was supported by the Japanese Ministry of Health, Labor, and Welfare; the KEIO Medical Association (Japan); and the National Childhood Cancer Foundation (United States).

Drs. Peuchmaur, d'Amore, Joshi, Hata, Roald, Dehner, and Shimada are members of the International Neuroblastoma Pathology Committee.

Address for reprints: Hiroyuki Shimada, M.D., Ph.D., Department of Pathology and Laboratory Medicine, Childrens Hospital Los Angeles, MS 43, 4650 Sunset Boulevard, Los Angeles, CA 90027; Fax: (323) 667-1127, E-mail: hshimada@chla.usc.edu

Received May 27, 2003; revision received August 4, 2003; accepted August 7, 2003.

DOI 10.1002/cncr.11773

BACKGROUND. Ganglioneuroblastoma, nodular (GNBn) comprises one of the categories of peripheral neuroblastic tumors. All tumors in this category, according to the original International Neuroblastoma Pathology Classification, are classified into an unfavorable histology group. Subsequently, it has been reported that GNBn can be divided into two prognostic subsets, a favorable subset (FS) and an unfavorable subset (US).

METHODS. Histology slides from 70 patients who were enrolled in Children's Cancer Group studies 3881 and 3891 and who had a diagnosis of GNBn were reviewed jointly by the members of International Neuroblastoma Pathology Committee (INPC): 1) to confirm the diagnosis of GNBn, 2) to identify the FS and US by applying the same age-linked criteria that were used to distinguish the favorable histology group and unfavorable histology group in conventional neuroblastoma tumors from the neuroblastomatous component of GNBn tumors, and 3) to verify the significant prognostic difference between these two subsets. The patients had been used in a previous study, and survival data for the patients were updated since the time of their last report.

RESULTS. The review clarified and illustrated morphologic characteristics of classical GNBn and it variants. The diagnosis of GNBn was confirmed in 67 of 70 patients. There were 22 patients with GNBn in the FS and 45 patients with GNBn in the US. The estimated survival differences between the FS and US patients with GNBn were statistically significant (8-year event free survival rate: 86.1% vs. 32.2%; $P = 0.0003$; overall survival rate: 90.5% vs. 33.2%; $P = 0.0003$).

CONCLUSIONS. This study confirmed the recently defined prognostic subsets of GNBn. The INPC proposes to modify the International Neuroblastoma Pathology Classification by distinguishing the FS and the US among patients with GNBn tumors. *Cancer* **2003;98:2274–81.** *© 2003 American Cancer Society.*

KEYWORDS: peripheral neuroblastic tumors; ganglioneuroblastoma, nodular; prognostic subsets; international classification; International Neuroblastoma Pathology Committee; histology.

Peripheral neuroblastic tumors (pNTs) constitute one of the most common solid tumors in infancy and early childhood. The International Neuroblastoma Pathology Classification (International Classification) proposed by the International Neuroblastoma Pathology Committee (INPC)[1–3] with the adoption of the original Shimada system[4,5] describes four categories of pNTs: neuroblastoma (Schwannian stroma-poor); ganglioneuroblastoma, intermixed (Schwannian stroma-rich); ganglioneuroma (Schwannian stroma-dominant); and ganglioneuroblastoma, nodular (composite: Schwannian stroma-rich/stroma-dominant and stroma-poor). According to the International Classification, morphologic features (grade of neuroblastic differentiation and mitosis-karyorrhexis index [MKI]) along with patient age at the time of diagnosis are taken into account for the prognostic distinction of neuroblastoma tumors into favorable histology (FH) or unfavorable histology (UH) groups. Tumors in the categories of ganglioneuroblastoma, intermixed and ganglioneuroma all are classified into an FH group, whereas all ganglioneuroblastoma, nodular (GNBn) tumors are classified into an UH group according to the International Classification and are considered to be associated with aggressive clinical behavior.[1,2,6]

In a recent study of 70 patients with GNBn by Umehara et al.,[7] however, two prognostic subsets, i.e., a favorable subset (FS) associated with relatively nonaggressive clinical behavior and a unfavorable subset (US) with aggressive clinical behavior, were delineated by applying to their neuroblastomatous (stroma-poor) component(s) the same age-linked morphologic criteria that were used for the prognostic distinction of conventional neuroblastoma tumors.[1,2] The aforementioned findings reported by Umehara et al.,[7] if confirmed, would require modification of the International Classification with respect to GNBn. Therefore, the members of INPC undertook a histopathology review of the same 70 patients with GNBn who were used in the report by Umehara et al. and made an analysis of prognostic effects by FS and US based on the updated follow-up information of the patients. The objectives of this article were 1) to clarify and illustrate the morphologic criteria of classical GNBn and its variants, 2) to report the results of the review that confirmed the findings of Umehara et al.,[7] and 3) to recommend a modification of the original International Classification with respect to GNBn.

MATERIALS AND METHODS

The materials used in this study consisted of tumors from 70 patients who were diagnosed originally with GNBn from Children's Cancer Group (CCG) studies 3881 and 3891 (from August 1991 to August 1995). The patients, the same group that was used in the report by Umehara et al.,[7] accounted for 9.7% of the pNTs in those CCG studies, with the remaining 90.3% (654 tumors) classified into the other categories (neuroblastoma; ganglioneuroblastoma, intermixed; and ganglioneuroma). Clinical information was derived from these protocols,[8–11] and the follow-up data have been updated by the Statistic Center at the CCG Operations Office (Arcadia, CA).

The pathology slides from these 70 tumors were from the repository of the CCG Neuroblastoma Pathology Center at the Department of Pathology and Laboratory Medicine, Childrens Hospital Los Angeles (Los Angeles, CA). The average number of hematoxylin and eosin-stained sections per tumor was 7 (range, 1–24 sections). Macroscopic data originally obtained from the institutional pathologists and confirmed by Umehara et al.[7] was used along with data from the histologic review.

The pathology review was conducted jointly using a multiheaded microscope by the members of INPC (E.S.G.d'A., J.H., V.V.J., M.P., B.R., and H.S.) without knowledge of clinical information or of the results found in the previous report by Umehara et al.[7] The review had multiple steps: i.e., 1) to verify the diagnosis of GNBn; 2) to identify the classical form of GNBn and its variants based on the nodular morphology of the stroma-poor neuroblastomatous component(s) (Fig. 1, Table 1); 3) to describe the histologic appearance of the stroma-rich/stroma-dominant component; and, finally, 4) to assign a prognostic subset to each tumor after evaluating the nodular histology of the given tumor by applying the age-linked morphologic features (for details, see the following paragraph). The consensus diagnoses were made by four of five or five of five agreements by the five member pathologists (E.S.G.d'A., J.H., V.F.J., M.P., and B.R.). H.S. did not participate in the voting for consensus diagnoses, because he had been involved in the study by Umehara et al. that used the same patients.

Nodular histology varied from tumor to tumor and even in the same tumor tissue. In many tumors, a single nodular histology with the same grade of neuroblastic differentiation and the same MKI class was seen throughout a single nodule or multiple nodules in the same tumor tissues. In some tumors, however, different nodular histologies were found in the different nodular lesions or even in a single nodular lesion

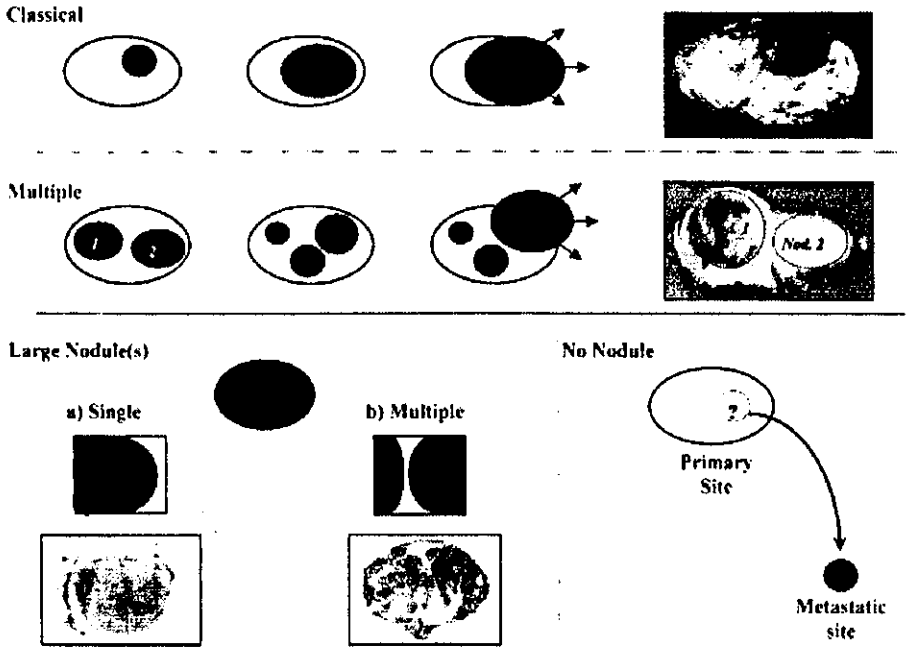

FIGURE 1. Ganglioneuroblastoma, nodular: classical form and variants (for details, see text).

TABLE 1
Ganglioneuroblastoma, Nodular and its Variants

	Criteria
Classical	Macroscopically visible neuroblastomatous (usually hemorrhagic) nodule in a ganglioneuromatous component with features of ganglioneuroblastoma, intermixed or ganglioneuroma of maturing or mature subtype in the tumor outside the nodule; on microscopic examination, there is abrupt transition between the neuroblastomatous nodule and the surrounding ganglioneuromatous component with or without a capsule (rarely focal invasion of former into latter may be seen); the neuroblastomatous component usually is of the undifferentiated or poorly differentiated subtype and rarely is of the differentiating subtype
Multiple nodules	Macroscopically visible, two or more neuroblastomatous nodules with a ganglioneuromatous component in the remaining portion of the tumor; the features of the nodules are the same as in the classical form
Large	No macroscopically visible nodules on a ganglioneuromatous battleground; the tumor nodule(s) resembles neuroblastoma on macroscopic examination; however, on microscopic examination, a ganglioneuromatous component is found as a thin rim at the periphery of large neuroblastomatous mass or as the trabecular portion between multiple neuroblastomatous nodules
No nodule	Primary tumor has features of ganglioneuroblastoma, intermixed or ganglioneuroma, but metastasis to lymph node, bone, or other site shows neuroblastomatous feature

from the same tumor. The morphologic features used for evaluation of the nodular histology were the same as those used for the prognostic distinction of conventional neuroblastoma (stroma-poor) tumors, and included grade of neuroblastic differentiation (undifferentiated, poorly differentiated, or differentiating) and mitosis karyorrhexis-index (MKI) (low MKI, $< 2\%$ or < 100 per 5000 cells; intermediate MKI, 2–4% or 100–200 per 5000 cells; high MKI, of $> 4\%$ or > 200 per 5000 cells). Table 2 shows that two different types of nodules, favorable nodules (FNs) and unfavorable nodules (UNs), were distinguished in the GNBn tumors. The FNs included 1) poorly differentiated or differentiating neuroblastoma with a low or intermediate MKI diagnosed in patients younger than 1.5 years; and 2) differentiating neuroblastoma with a low MKI diagnosed in children ages 1.5–5.0 years. The UNs included 1) any neuroblastoma with a high MKI at any age, 2) any neuroblastoma with an intermediate MKI in children older than 1.5 years, 3) undifferentiated neuroblastoma at any age, 4) poorly differentiated neuroblastoma diagnosed in children older than 1.5 years, and 5) any neuroblastoma diagnosed in children age > 5.0 years. After nodular histology was determined, the GNBn tumors were classified into two prognostic subsets. The FS of GNBn included tumors that contained single or multiple FNs. The US included tumors with single UNs or multiple nodules that contained at least one UN.

Statistical analyses were performed by using the

TABLE 2
Prognostic Evaluation for Nodular Component of Ganglioneuroblastoma, Nodular[a]

Nodular component	Description
Favorable nodules	
Age < 1.5 yrs	Poorly differentiated or differentiating and low or intermediate MKI tumor
Age 1.5–5.0 yrs	Differentiating and low MKI tumor
Unfavorable nodules	
Age < 1.5 yrs	1) Undifferentiated tumor; 2) high MKI tumor
Age 1.5–5.0 yrs	1) Undifferentiated or poorly differentiated tumor; 2) intermediate or high MKI tumor
Age > 5.0 yrs	All tumors

MKI: mitosis-karyorrhexis index.
[a] The criteria used were same as the Shimada system criteria for the prognostic distinction of conventional neuroblastoma tumors according to the International Neuroblastoma Pathology Classification.

two-sided Pearson chi-square test or a two-sample *t* test for comparing histopathologic, clinical, and biologic characteristics of FS and US in the GNBn tumors. The prognoses for patients in the two subsets were evaluated, and their estimated event-free survival (EFS) and overall survival (OS) experience were calculated using the Kaplan–Meier method.[12]

RESULTS

Pathology Review of Tumors in the GNBn Category

The diagnosis was confirmed in 67 of 70 tumors that originally were considered GNBn by Umehara et al.[7] One of the three rejected tumors was diagnosed as neuroblastoma by the INPC review, and there was a limited and ambiguous, small area of ganglioneuromatous component intermingled with the stroma-poor tumor tissue. The other two tumors were considered indeterminate types of NT by the review: Although two distinctively separated and well demarcated neuroblastomatous components were present, one that was less differentiated and the other that was more differentiated, neither of them showed a ganglioneuromatous appearance. These two tumors—one with a feature of *stroma-poor, differentiating subtype with a low MKI* component accompanied by a hemorrhagic nodular lesion of *stroma-poor, poorly differentiated subtype with an intermediate MKI* component (diagnosed at age 4 years and 4 months with Stage IV disease; the patient died of tumor), and the other with a feature of *stroma-poor, differentiating subtype with low MKI* component accompanied by a hemorrhagic, nodular lesion of *stroma-poor, poorly differentiated subtype with a low MKI* component (diagnosed at the age of 2 years and 2 months with Stage IV disease; the patient died of tumor), could be termed *nodular neuroblastoma*, which awaits further definition and characterization with accumulation of more tumors with comparable features.

Among 67 patients, 61 patients had macroscopically identifiable nodule(s) in the primary tumors: Twenty were classical GNBn with a single nodule (single-nodular tumors), 33 were considered variants with two or more nodules (multiple-nodular tumors), and the number of nodules was not determined in eight tumors. The remaining six tumors also were considered as variant: Four tumors were of large-nodule type and were comprised predominantly of a stroma-poor component without a macroscopically recognizable stroma-rich/stroma-dominant component, and two tumors had a ganglioneuroma (Schwannian stroma-dominant) histology in the primary site and a neuroblastoma (Schwannian stroma-poor) histology in metastatic lesion to the bone.

The histologic features (grade of neuroblastic differentiation and MKI) of the stroma-poor components of the 67 fully analyzed tumors are summarized in Table 3. With regard to the Schwannian stroma-rich/stroma-dominant component, 45 tumors (67.2%) showed ganglioneuroblastoma, intermixed morphology; whereas 22 tumors (32.8%) displayed ganglioneuroma, maturing (19 patients) or mature (3 patients) morphology.

Prognostic Subsets of GNBn

The review by INPC members confirmed the findings reported by Umehara et al.[7] There were 22 patients (32.8%) who had GNBn with features of FS and 45 patients (67.2%) who had GNBn with features of US in the neuroblastomatous component(s). The nodules that were made up of a single histology (n = 59 patients) were classified either as FS (21 of 59 patients; 35.59%) or US (38 of 59 patients; 64.4%) because of the presence of FNs or UNs, respectively. Histologically different nodular components that were found in the same primary tumor tissue (n = 8 patients) were evaluated separately: A tumor with FN/FN (one patient) was classified as FS, and tumors with FN/UN (5 patients) and UN/UN (2 patients) were classified as US (Table 3). Table 4 shows that the US was found more frequently in the variant GNBn tumors (30 of 39 tumors; 76.92%) compared with the classical GNBn tumors (8 of 20 tumors; 40%; P = 0.005). Figure 2 demonstrates that the expected 8-year OS and EFS rates for the US patients with GNBn subtype tumors (33.2% and 32.2%, respectively) were significantly lower compared with the FS patients with GNBn subtype tumors (90.5% and 86.1%, respectively; P = 0.0003).

The clinical characteristics of these two subsets are summarized in Table 5. It was noted that children with US tumors were significantly older than children

TABLE 3
Histologic Features of the Nodule in the 67 Ganglioneuroblastomas, Nodular

Histologic feature	SH	DH	FS	US	Total
Single nodular classic (n = 20) and large nodular variants (n = 4)	22	2			24
Poorly diff. and low MKI	—[a]		3	8	11
Poorly diff. and intermediate MKI	—[a]		1	1	2
Poorly diff. and high MKI	—[a]		0	2	2
Diff. and low MKI	—[a]		7	0	7
Poorly diff. and low MKI (FS); diff. and low MKI (FS)		—[b]	1	0	1
Poorly diff. and intermediate MKI (US); diff. and low MKI (FS)		—[b]	0	1	1
Multiple nodular variants (n = 33)	27	6			33
Undiff. and low MKI	—[a]		0	1	1
Poorly diff. and low MKI	—[a]		3	12	15
Poorly diff. and intermediate MKI	—[a]		0	3	3
Poorly diff. and high MKI	—[a]		0	2	2
Diff. and low MKI	—[a]		6	0	6
Poorly diff. and low MKI (FS); poorly diff. and high MKI (US)		—[b]	0	1	1
Poorly diff. and low MKI (US); poorly diff. and high MKI (US)		—[b]	0	1	1
Diff. and low MKI (FS); poorly diff. and low MKI (US)		—[b]	0	2	2
Diff. and low MKI (FS); poorly diff. and intermediate MKI (US)		—[b]	0	1	1
Diff. and low MKI (US); poorly diff. and low MKI (US)		—[b]	0	1	1
No. of nodules unknown (n = 10)	10				10
Undiff. and low MKI	—[a]		0	1	1
Poorly diff. and low MKI	—[a]		0	4	4
Poorly diff. and intermediate MKI	—[a]		0	2	2
Diff. and low MKI	—[a]		1	0	1
Ganglioneuroma with bone metastasis, variants (poorly diff.)[c]	—[a]		0	2	2
Total			22	45	67

SH: single histology; DH: double histologies; FS: favorable subset; US: unfavorable subset; undiff.: undifferentiated; poorly diff. poorly differentiated; diff.: differentiating; MKI: mitosis-karyorrhexis index.

[a] Single histology.

[b] Double histologies.

[c] In these patients, the histology of the bone metastasis along with the age (older than 4 years) justified the unfavorable categorization regardless of the mitosis-karyorrhexis index, which could not be determined.

TABLE 4
Classical Ganglioneuroblastoma, Nodular and Variants

Morphology	FS	US	Total
Classical[a]	12	8	20
Variants			
Multiple	9	24	33
Large nodule(s)[b]	0	4	4
No nodule[c]	0	2	2
No. of nodules unknown	1	7	8
Total	22	45	67

FS: favorable subset; US: unfavorable subset.

[a] A single, macroscopically visible, nodular formation that was detected by macroscopic examination.

[b] A ganglioneuromatous component that was not detected by macroscopic examination.

[c] No nodule was detected in the primary tumor with bone metastasis.

with FS tumors (97.8% vs. 59.1% diagnosed after age 1.5 years; 31.1% vs. 0.0% diagnosed after age 5.0 years). FS tumors were distributed evenly in various clinical stages, whereas patients with US tumors frequently presented (63.0%; 29 of 46 patients) with distant metastases (Stage IV). No significant difference was found in primary distribution sites between the subsets.

With regard to the stroma-rich/stroma-dominant component, tumors with ganglioneuroma (Schwannian stroma-dominant) morphology were found in significantly older children (age, 5.72 ± 3.66 years) compared with children who had ganglioneuroblastoma, intermixed (Schwannian stroma-rich) morphology (age, 3.29 ± 3.09 years; $P < 0.005$). It is noteworthy that tumors with ganglioneuroma morphology almost always had the UN component (20 of 22 tumors; 90.9%), whereas slightly more than 50% of tumors with ganglioneuroblastoma, intermixed morphology (55.55%; 25 of 45 tumors) had the UN component ($P = 0.005$).

DISCUSSION

Since its original description by Stout in 1947,[13] GNBn usually has been considered an unfavorable tumor with low EFS and OS.[1–6,14,15] GNBn tumors are considered molecularly heterogeneous[16]: the stroma-rich component represents a biologically nonaggressive clone, whereas the neuroblastomatous clone(s) accounts for the poor prognosis. However, the results of the study by Umehara et al.[7] challenged this belief and showed that the neuroblastomatous components in this category of pNTs were not always aggressive. The current study by the INPC confirmed the conclusions drawn by Umehara et al.,[7] and the prognosis of patients with GNBn was determined by precise evaluation of histology, applying the same age-linked criteria that are used for conventional neuroblastomas (Schwannian stroma-poor tumors) to the nodular components. Two distinct prognostic subsets, FS and US, were identified in the GNBn category. Tumors in the FS category were comprised of a Schwannian stroma-rich/stroma-dominant component and the FN component, and the patients had significantly better EFS and OS rates compared with children who had US tumors. In contrast, the US tumors contained UN and behaved aggressively, with frequent distant metastasis at the time of diagnosis.

With these results, the INPC clearly defined the

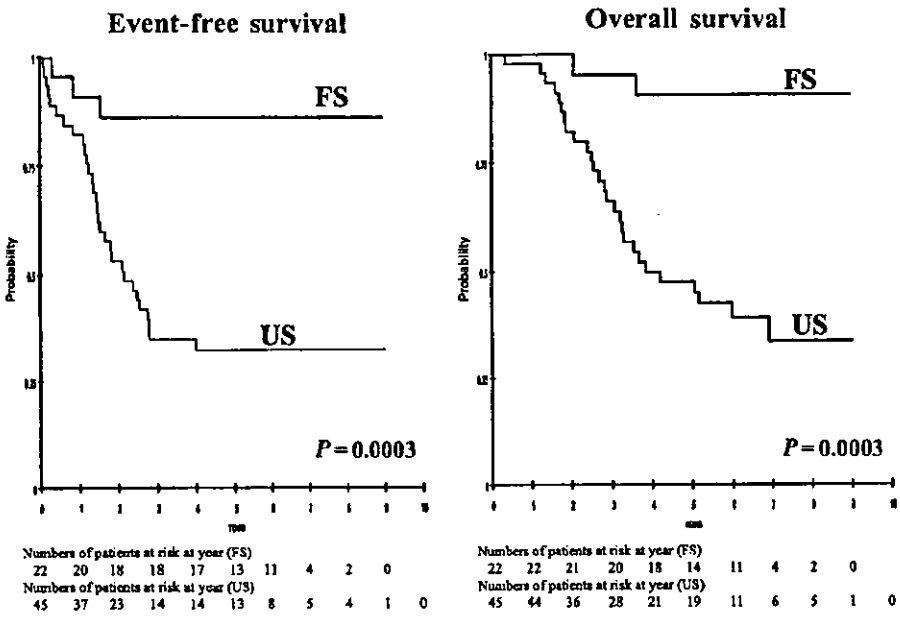

FIGURE 2. Event-free survival (EFS) curves and overall survival (OS) curves for patients with ganglioneuroblsatoma, nodular (GNBn) in the favorable subset (FS) and the unfavorable subset (US). The 8-year expected EFS and OS rates differed significantly between these two prognostic subsets of patients: 86.1% and 90.5% for patients in the FS group and 32.2% and 33.2% for patients in the US group, respectively ($P < 0.0003$).

TABLE 5
Clinical Summary of 67 Patients

Feature	No. of patients (%) FS	US	P value
CCG study			
CCG 3881	18 (81.8)	12 (26.7)	< 0.0001
CCG 3891	4 (18.2)	33 (73.3)	
Survival (8 yrs)	90.50%	33.20%	0.0003
Event free survival (8 yrs)	86.10%	32.10%	0.0003
Age			
< 1.5 yrs	9 (40.9)	1 (2.2)	< 0.001
1.5–5.0 yrs	13 (59.1)	30 (66.7)	
> 5.0 yrs	0 (0.0)	14 (31.1)	
Clinical stage			< 0.05
I	4 (18.2)	2 (4.4)	
II	7 (31.8)	9 (20.0)	
III	6 (27.3)	6 (13.3)	
IV	5 (22.7)	28 (62.2)	
Primary site			NS
Chest	9 (40.9)	11 (24.4)	
Thoracoabdominal	0 (0.0)	1 (2.2)	
Adrenal	7 (31.8)	20 (44.4)	
Abdomen	4 (18.2)	8 (17.8)	
Pelvis	2 (9.1)	4 (8.9)	
Others	0 (0.0)	1 (2.2)	
Schwannian stroma-rich/stroma-dominant histology			
Ganglioneuroblastoma, intermixed	20 (90.9)	25 (55.6)	< 0.005
Ganglioneuroma	2 (9.1)	20 (44.4)	
Total	22 (100)	45 (100)	

FS: favorable subset; US: unfavorable subset; CCG: Children's Cancer Group; NS: not significant.

concept of GNBn as a composite tumor comprised of a favorable stroma-rich/stroma-dominant component and nodular component(s) of either a biologically favorable clone, an unfavorable clone, or both clones: A single clone could be either FN or UN, whereas multiple clones could be FN/FN, FN/UN, or UN/UN. The presence of any UN, either as a single nodule (UN) or in multiple nodules (FN/UN and UN/UN), indicates an aggressive behavior of the given GNBn tumor and indicates a poor clinical outcome for the patient.

The morphology of GNBn as well as the proportion of stroma-rich/stroma-dominant components and stroma-poor components in the same tumor tissue seem to vary depending on their natural history and the time of surgery/diagnosis. The FN component, although it is less mature morphologically compared with the stroma-rich/stroma-dominant component in the same tumor tissue, is expected to have potential for differentiation and, thus, well may belong in the age-matched maturational sequence of biologically favorable pNTs defined by the Shimada system.[1–3] In contrast, the UN component can keep growing even after the ganglioneuromatous component (ganglioneuroblastoma, intermixed and ganglioneuroma) stops growing. These UNs in the GNBn category would remain unfavorable histopathologically, regardless of patient age. This may be one of the reasons why more FS tumors than US tumors are diagnosed in younger children. It also may explain the fact that the vast majority of tumors in older children

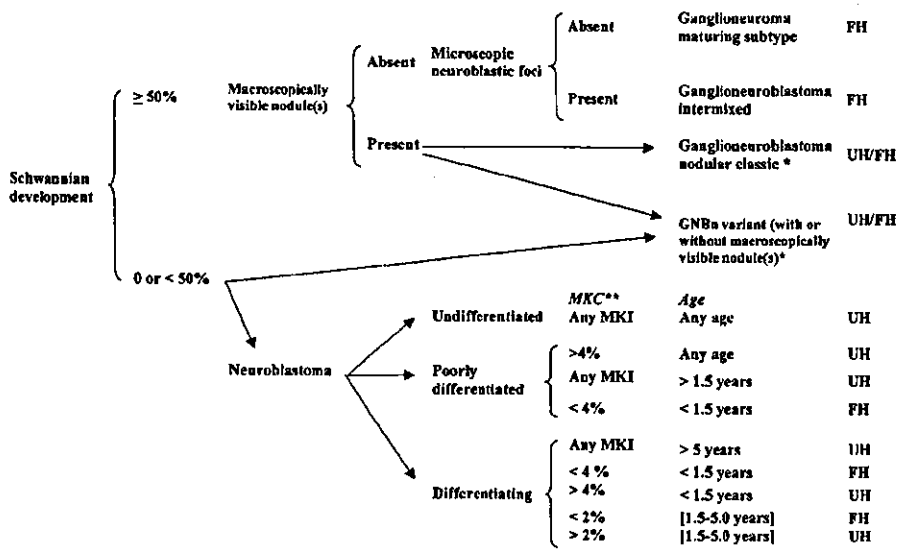

FIGURE 3. International Neuroblastoma Pathology Classification. FH: favorable histology; UH: unfavorable histology. GNBn: ganglioneuroblastoma, nodular; MKC: mitotic and karyorrhectic cells; MKI: mitosis-karyorrhexis index. Single asterisk: for a prognostic evaluation of GNBn, see text and Umehara et al.[7]; double asterisks: MKC: 2%, 100 of 5000 cells, 4%, 200 of 5000 cells.

that had ganglioneuroma (Schwannian stroma-dominant) morphology did not have FNs.

In two patients, a neuroblastomatous component was found in the metastatic site but was not identified in the primary tumor. Because of neuroblastomatous components that placed both of these patients in the US, sampling error of the unfavorable clone, possibly due to its small size, was suspected rather than its spontaneous regression or maturation in the primary site.

Therefore, it is recommended by the INPC that two prognostic subsets of GNBn should be recognized. Accordingly, the International Classification needs to be modified, and two prognostic subsets—i.e., FS and US, should be included in the GNBn category, although the INPC criteria for prognostic classification of neuroblastoma; ganglioneuroblastoma, intermixed; and ganglioneuroma remain the same (Fig. 3).

It also needs to be emphasized that pathologists should be aware of all GNBn variants and should familiarize themselves with their morphologic features. It should be noted here that classical GNBn, comprised of a single, macroscopically visible, usually hemorrhagic nodule in a background of stroma-rich/stroma-dominant tissue, was determined in only 20 of 67 patients (30%) in this series. Careful macroscopic examination of the resected mass, including multiple sampling from the periphery of the tumor and from the periphery of the vague or definite nodule(s) seen on macroscopic examination, is essential and critical for the recognition of GNBn variants. Pathologists also should be aware that the nodular histology of GNBn may vary from one nodule to another in multiple-nodular tumors and even in different microscopic fields of the same nodule of either single-nodular or multiple-nodular tumors. Histologically different nodules or areas in the same tumor need to be evaluated separately and individually for determination of UN or FN status.

REFERENCES

1. Shimada H, Ambros IM, Dehner LP, Hata J, Joshi VV, Roald B. Terminology and morphologic criteria of neuroblastic tumors. Recommendations by the International Neuroblastoma Pathology Committee. *Cancer.* 1999;86:349–363.
2. Shimada H, Ambros IM, Dehner LP, Hata J, Joshi VV, Roald B, et al. The International Neuroblastoma Pathology Classification (the Shimada System). *Cancer.* 1999;86:364–372.
3. Joshi VV. Peripheral neuroblastic tumors: pathologic classification based on recommendations of International Neuroblastoma Pathology Committee (modification of Shimada classification). *Pediatr Dev Pathol.* 2000;3:184–189.
4. Shimada H, Chatten J, Newton WA, et al. Histopathologic prognostic factors in neuroblastic tumors: definition of subtypes of ganglioneuroblastoma and age-linked classification of neuroblastomas. *J Natl Cancer Inst.* 1984;73:405–416.
5. Joshi VV, Cantor AB, Altshuler G, et al. Recommendations for modification of terminology of neuroblastic tumors and prognostic significance of Shimada classification. *Cancer.* 1992;69:2183–2196.
6. Shimada H, Umehara S, Monobe Y, et al. International Neuroblastoma Pathology Classification for prognostic evaluation of patients with peripheral neuroblastic tumors: a report from the Children's Cancer Group. *Cancer.* 2001;92:2451–2461.
7. Umehara S, Nakagawa A, Matthay KK, et al. Histopathology defines prognostic subsets of ganglioneuroblastoma, nodular. *Cancer.* 2000;89:1150–1161.
8. Matthay KK, Perez C, Seeger RC, et al. Successful treatment of Stage III neuroblastoma based on prospective biologic staging: a Children's Cancer Group Study. *J Clin Oncol.* 1998;16:1256–1264.

9. Matthay KK, Villablanca JG, Seeger RC, et al. Treatment of high-risk neuroblastoma with intensive chemotherapy, radiotherapy, autologous bone marrow transplantation, and 13-cis-retinoic acid. Children's Cancer Group. *N Engl J Med.* 1999;341:1165–1173.
10. Nickerson HJ, Matthay KK, Seeger RC, et al. Favorable biology and outcome of Stage IV-S neuroblastoma with supportive care or minimal therapy: a Children's Cancer Group study. *J Clin Oncol.* 2000;18:477–486.
11. Perez CA, Matthay KK, Atkinson JB, et al. Biologic variables in the outcome of Stage I and II neuroblastoma treated with surgery as primary therapy: a Children's Cancer Group study. *J Clin Oncol.* 2000;18:18–26.
12. Kaplan EL, Meier P. Nonparametric estimation from incomplete observation. *J Am Stat Assoc.* 1958;53:457–481.
13. Stout AP. Ganglioneuroma of the sympathetic nervous system. *Surg Gynecol Obstet.* 1947;84:101–110.
14. Joshi VV, Cantor AB, Altshuler G, et al. Conventional versus modified morphologic criteria for ganglioneuroblastoma. A review of cases from the Pediatric Oncology Group. *Arch Pathol Lab Med.* 1996;120:859–865.
15. Adam A, Hochholzer L. Ganglioneuroblastoma of the posterior mediastinum: a clinicopathologic review of 80 cases. *Cancer.* 1981;47:373–381.
16. Schmidt ML, Salwen HR, Chagnovich D, Bauer KD, Crawford SE, Cohn SL. Evidence for molecular heterogeneity in human ganglioneuroblastoma. *Pediatr Pathol.* 1993;13:787–796.

Pathology International 2003; **53**: 214–220

Original Article

Responsiveness of chemotherapy based on the histological type and Wilms' tumor suppressor gene mutation in bilateral Wilms' tumor

Rie Shibata,[1] Ayako Takata,[1] Akinori Hashiguchi,[1] Akihiro Umezawa,[1] Taketo Yamada[1] and Jun-ichi Hata[1,2]

[1]*Department of Pathology, Keio University School of Medicine, and* [2]*National Research Institute for Child Health and Development, Tokyo, Japan*

To clarify a characteristic of bilateral Wilms' tumor (WT), we examined the clinical and histological features, chemotherapy response and mutations in Wilms' tumor suppressor gene (*WT1*) in five patients. Deoxyribonucleic acid was extracted from peripheral lymphocytes and tumor samples, and direct DNA sequencing was performed to detect *WT1* mutations. Paraffin sections were stained with H&E for histological review and immunostained with anti-*WT1*, anti-Ki-67, anti-S-100 protein and antimyogenin antibodies. In contrast to the single case of epithelial-type WT, the other four cases were fetal rhabdomyomatous nephroblastoma (FRN) or contained a premature skeletal muscle component and appeared to be resistant to chemotherapy because there was no reduction in tumor volume. However, after chemotherapy, most of the tumor components changed into mature striated muscle cells, most of which immunostained almost completely negative for Ki-67. All four cases had the same point mutation of *WT1*. From our results, the histological findings correlated with *WT1* mutations in bilateral WT. The tumor volume of FRN did not decrease in response to chemotherapy. It is possible to predict the chemotherapy response by examining bilateral WT for *WT1* mutations and the histological characteristics of tumors.

Key words: chemotherapy, fetal rhabdomyomatous nephroblastoma, Wilms' tumor, Wilms' tumor suppressor gene

Wilms' tumor (WT) is the most common malignant neoplasm of the kidney in childhood, accounting for approximately 8% of all childhood solid tumors, and 5–10% of WT patients present with bilateral disease.[1,2] Pathologically, bilateral WT tends to be fetal rhabdomyomatous nephroblastoma (FRN), a histological variant of WT characterized by a predominance of rhabdomyogenic components. Clinically, WT of the FRN type presents as a huge mass in younger patients. The tumor rarely metastasizes or shows aggressive behavior, and it has a good prognosis.[3] On the other hand, FRN is known to be resistant to the chemotherapy used to treat classical WT.[4,5] The Wilms' tumor suppressor gene (*WT1*) at chromosome 11p13 was identified in 1990, and it encodes a transcriptional factor containing a domain of four zinc finger motifs.[6,7] Schumacher *et al.* reported finding *WT1* mutations in four of the five cases of bilateral WT that they analyzed,[8] a much higher incidence than in sporadic WT.[1,2] Bilateral WT is explained by the two-hit mechanism of inactivation of tumor suppressor genes proposed by Knudson and Strong.[8–10] Because a germ line mutation in *WT1* has been reported to predispose the development of tumors with stromal-predominant histology,[8] the *WT1* mutation should be found in bilateral WT, especially the FRN histological subtype. However, there have been no reports discussing correlations between the histology of WT, the chemotherapy response and *WT1* mutations.

This report summarizes the clinical and pathological features in five cases of bilateral WT. This study analyzed the *WT1* gene mutation and attempted to determine why they are resistant to chemotherapy.

MATERIALS AND METHODS

Patients

Five patients with bilateral WT who underwent surgery between 1998 and 2001 were studied. Cases 2–5 were accompanied by genitourinary tract malformations (Table 1).

Correspondence: Jun-ichi Hata, MD, National Research Institute for Child Health and Development, 3-35-31 Taishido, Setagaya-ku, Tokyo 154-8567, Japan. Email: jhata@nch.go.jp

Received 19 September 2002. Accepted for publication 6 December 2002.

Table 1 Clinical and histological features and results of *WT1* mutations

Case	Age/Sex	Anomaly	Histology before chemotherapy	First chemotherapy	Tumor volume after therapy	Histological subtype after chemotherapy	Mutations germ line	Mutations tumor	Outcome
1	9 months/F	–	Epithelial type	V+A	Decrease	Epithelial type	–	–	Disease-free postoperative status
2	11 months/M	Cryptorchidism	FRN	V+A+D†	Increase	FRN	1168C→C/T	1168X→T(R390X)	Disease-free postoperative status
3	9 months/F	Cryptorchidism hypospadias	Nephroblastic-type striated muscle (+)	V+A†	Regression (-)	FRN	1168C→C/T	1168X→T(R390X)	Disease-free postoperative status
4	7 months/F	Ovarian dysgenesis	FRN	V+A†	Increase	FRN	1168C→C/T	1168X→T(R390X)	Disease-free postoperative status
5	1 year/M	Cryptorchidism	Nephroblastic-type striated muscle (+)	V+A†	Increase	Nephroblastic-type striated muscle cells: increase	1168C→C/T	1168X→T(R390X)	Under treatment

†Additional aggressive chemotherapy was performed. A, actinomycin; C, cytosine; D, doxorubicin; FRN, fetal rhabdomyomatous nephroblastoma; T, thymine; V, vincristine.

Cases 2 and 5 were associated with cryptorchidism, case 3 with bilateral cryptorchidism and hypospadias, and case 4 with left ovarian dysgenesis. None of the patients showed evidence of renal dysfunction or renal failure. Fresh tumor tissue and peripheral blood samples were obtained from all five patients when tumorectomy was performed. The clinical features of the patients are summarized in Table 1. Informed consent was obtained from all patients or their parents.

Histopathological analysis

The biopsy specimens before chemotherapy and the resected tumors after chemotherapy were fixed with 10% formalin and embedded in paraffin. Paraffin sections were stained with H&E. Histological subtyping of WT was performed according to the classification proposed by the Japanese Society of Pathology, [11] and FRN was defined as more than 1/3 of the tumor mass showing striated muscle differentiation. However, the nephroblastic type of tumor was defined as the tumor that showed triphasic histology containing striated muscle, but its proportion of the tumor was less than 1/3.[11] We used biopsied specimens to diagnose the histology of tumors before chemotherapy. All five cases underwent open biopsy and we took them to represent the histology of tumor. Some sections were subjected to immunohistochemistry for WT1, Ki-67, myogenin and S-100 protein by the avidin-biotin-peroxidase technique using anti-WT1 antibody (dilution 1:200; DAKO, Carpinteria, CA, USA), anti-Ki-67 antibody (dilution 1:500; DAKO, Kyoto, Japan), antimyogenin antibody (dilution 1:200; Santa Cruz, CA, USA) and anti-S-100 protein antibody (dilution 1:2000; DAKO, Japan). For WT1 staining, deparaffinized and rehydrated sections were treated with 0.4% pepsin in 0.2 NHCl for 30 min at 37°C before reacting with anti-WT1 antibody. Deparaffinized and rehydrated sections were heated at 100°C in 0.01 mol/L sodium citrate buffer (pH 6.0) for 10 min before reacting with anti-Ki-67 and antimyogenin antibody.

DNA preparation

The DNA was extracted from leukocytes and tumor tissue by the sodium dodecyl sulfate-proteinase K method with slight modifications, as described previously.[12] Amplification of exons 1–10 was performed by polymerase chain reaction (PCR). Direct sequencing of the PCR products was performed with a MegaBACE 1000 DNA Sequencing System (Amersham Biosciences, Florida, USA). The precise methods have been described previously.[12] The PCR and sequence primers we used are shown in Table 2. All procedures were approved by the Ethical Committee of the Keio University School of Medicine.

Table 2 Polymerase chain reaction (PCR) and sequence primers

exon	Name	PCR sequence	Name	Sequence
1	WT256	AGCCAGAGCAGCAGGGAGTC	SEQ1-S	GGCATCTGGGCCAAGTTAGG
	WTEX1R2	CGGTCAAAAGGGGTAGGAGA	SEQ1-A	CCTAGAGCGGAGAGTCCCTG
2	2B-S	TGGCTGGTTCAGACCCACTG	SEQ2-S	TGCCCCGTCTTGCGAGAGCA
	2B-A	AGAGGAGGATAGCACGGAAG	SEQ2-A	GCACGGAAGAAGGGGAGAAG
3	3B-S	CCAGGCTCAGGATCTCGTGT	SEQ3-S	ATCTCGTGTCTCCCCCAACC
	3B-A	GGCGTCTCGTGCCTCCAAGA	SEQ3-A	GTGCCTCCAACACCCTGCAT
4	4B-S	TGTGGAGGCTTGCACTTTCA	SEQ4-S	GAAGAAACAGTTGTGTATTATTTTG
	4B-A	GCCCTTTCTTCTAAAACTGT	SEQ4-A	ATGGTTCAAACAGGTATAAGTTACT
5	5B-S	TCACTGGATTCTGGGATCTG	SEQ5-S	CTGGGATCTGGGGGGCTTGCCA
	5B-A	AGTCCTAACTCCTGCATTGC	SEQ5-A	CCCCAGGTGCCAGTCAGCAAGG
6	6B-S	AAAACCATCATTCCCTCCTG	SEQ6-S	TTTCCAAATGGCGACTGTGAGC
	6B-A	CAAAGAGTCCATCAGTAAGG	SEQ6-A	GGTAAGTAGGAAGAGGCAGTGC
7	7F-S	GTGCTCACTCTCCCTCAAGA	SEQ7-S	TCCCTCAAGACCTACGTGAATGTTC
	7F-A	GTGAGAGCCTGGAAAAGGAGC	SEQ7-A	TTGAACCATGTTTGCCCAAGACTGG
8	8-S	AGATCCCCTTTTCCAGTATC	SEQ8-S	AGATCCCCTTTTCCAGTATC
	8C'-A	CAACAACAAAGAGAATCA	SEQ8-A	AAATCAACCCTAGCCCAAGG
9	9C-S	AAGTCAGCCTTGTGGGCCTC	SEQ9-S	CCCACATTGGTTAGGGCCGAGGCTA
	9C-A	TTTCCAATCCCCTCTCATCAC	SEQ9-A	TAGGGCCGAGGCTAGACCTTCTCT
10	10C-S	CACTCGGGCCTTGATAGTTG	SEQ10-S	TTTCCAATCCCCTCTCATCAC
	10C-A	GTCAGACTTGAAAGCAGTTC	SEQ10-A	TGTGCCTGTCTCTTTGTTGC

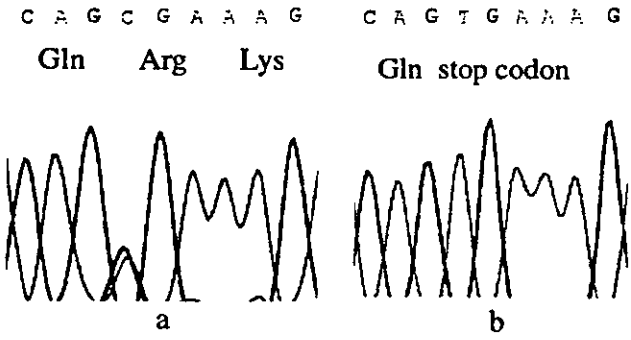

Figure 1 Results of the DNA sequence analyses of germ line (**a**) and tumor samples (**b**). (**a**) A heterozygous point mutation, 1168 cytosine/thymine, was found in exon 9 in the germ line in cases 2–5. (**b**) A point mutation, 1168C/T, converts the codon for 390Arg into a stop codon in the tumors in cases 2–5.

RESULTS

The clinical and pathological features and results of *WT1* mutations are summarized in Table 1. The DNA sequence analyses indicated the same point mutations at exon 9 in cases 2–5. The mutation was a cytosine to a thymine substitution in zing finger 3 and resulted in a ^{390}Arg becoming a stop codon (R390X). There was a heterozygous mutation at the same codon in the germ line of all four patients (Fig. 1). No *WT1* mutation was detected in case 1.

The histological subtype in case 1 was the epithelial type, and the specimens before chemotherapy contained no clear striated muscle components. Cases 2 and 4 showed the typical histological features of FRN. Cases 3 and 5 were nephroblastic type and contained abundant striated muscle components before chemotherapy.

Only case 1 was responsive to chemotherapy consisting of vincristine and actinomycin D. As the tumor volume in the other cases either increased (cases 2, 4, and 5) or was unchanged (case 3), additional aggressive chemotherapy was carried out in these four cases, but tumor regression did not occur regardless of the chemotherapy regimen. Finally, all patients underwent bilateral tumorectomy. Cases 1–4 are disease-free after tumorectomy. In case 5, tumor rupture occurred during chemotherapy, and the patient is now on chemotherapy after bilateral nephrectomy.

Histological examination of all resected tumors after chemotherapy, except in case 1, showed a predominance of mature striated muscle and collagenous tissue (Fig. 2). The epithelial and blastemal components of cases 2–5 were markedly reduced in the tumor tissue. However, we diagnosed case 3 as nephroblastic type before chemotherapy because almost the entire tumor was composed of striated muscle components after chemotherapy. Therefore, we diagnosed case 3 as an FRN-like tumor after chemotherapy. The resected tumor of case 1 contained no striated muscle or collagen fibers. None of the tumors examined showed histological anaplasia before or after chemotherapy.

Before chemotherapy, the striated muscle cells were positive for myogenin, a protein that regulates the differentiatin of myogenic cells and is expressed in the cells induced to differentiate (Fig. 3a), and they were negative for S-100 protein, which is expressed in mature skeletal muscles (Fig. 3b). After chemotherapy, mature striated muscle was negative for myogenin (Fig. 3c) and positive for S-100 protein (Fig. 3d). Ki-67 was positive in the nuclei of almost all of the tumor cells

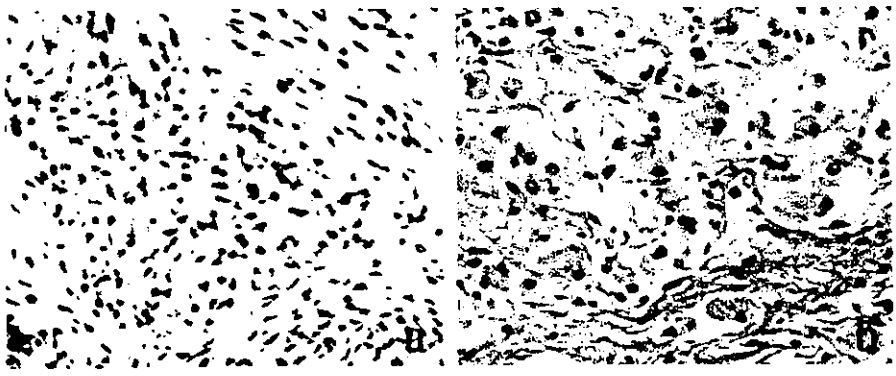

Figure 2 H&E section from case 4. (a) Preoperative biopsy. Immature striated muscle is the predominant stromal element. (original magnification, ×100) (b) Resected tumor after chemotherapy. The components are mostly mature striated muscle and collagen fiber. (original magnification, ×100)

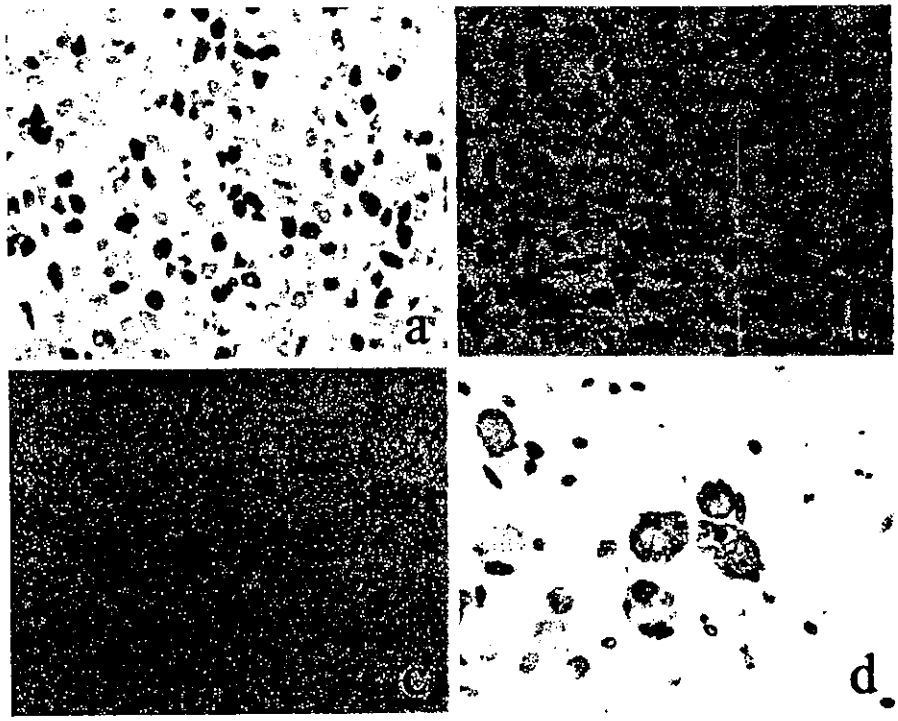

Figure 3 Immunohistochemical analysis of sections from case 4 with myogenin and S-100 protein (original magnification, ×200) (a) Striated muscle cells before chemotherapy are positive for myogenin, a protein that regulates myogeninc cell differentiation and is expressed in cells induced to differentiate. (b) Tumor cells before chemotherapy are negative for S-100 protein, expressed in mature skeletal muscle. (c) Striated muscle cells after chemotherapy are negative for myogenin. (d) Striated muscle cells after chemotherapy are positive for S-100 protein.

before chemotherapy (Fig. 4a), but the mature striated muscle cell components were almost negative for Ki-67 (Fig. 4b). The epithelial and blastemal components of the tumors were positive for Ki-67 (data not shown). The tumors in cases 2–5 that carried the *WT1* point mutation were negative for *WT1* staining (Fig. 5a), whereas case 1, which did not have the *WT1* mutation, was positive for immunostaining (Fig. 5c).

DISCUSSION

In this report, we have summarized the clinical course and histological features in five cases of bilateral WT before and after chemotherapy. We also demonstrated a *WT1* mutation in them. Our results support that loss of *WT1* expression as a result of *WT1* mutation is correlated with the histological features of WT.[8] They also suggest that histological features are related to the response of chemotherapy. As unilateral WTs are usually resected before chemotherapy according to the Japan Wilms' Study Group protocol, it is difficult to compare histological features before and after chemotherapy. The estimated incidence of *WT1* mutation in unilateral or sporadic WT cases is approximately 10–15%.[2] We consider it important to clarify the histological features and response to chemotherapy in bilateral WTs carrying *WT1* mutations with higher incidence than unilateral WTs.

Cases 2–5 were found to have the same point mutations, a change from C to T in zing finger 3, resulting in ^{390}Arg becoming a stop codon. During translation, this nonsense mutation leads to protein truncation, with the result that the last zing finger necessary for DNA binding of *WT1* is missing. Interrupted DNA binding to the target genes of *WT1* fusion

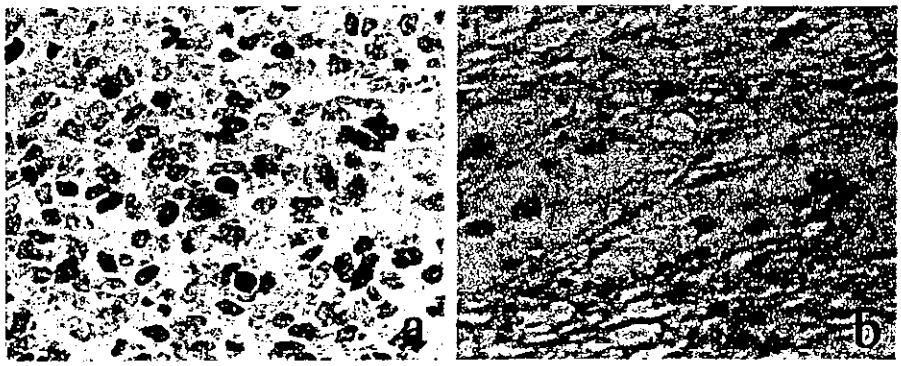

Figure 4 Immunohistochemical analysis of Ki-67 (original magnification, ×400) (**a**) Preoperative biopsy of Case 3. Tumor cells are positive for Ki-67 before chemotherapy. (**b**) Resected tumor of case 3. Tumor tissue is negative for Ki-67.

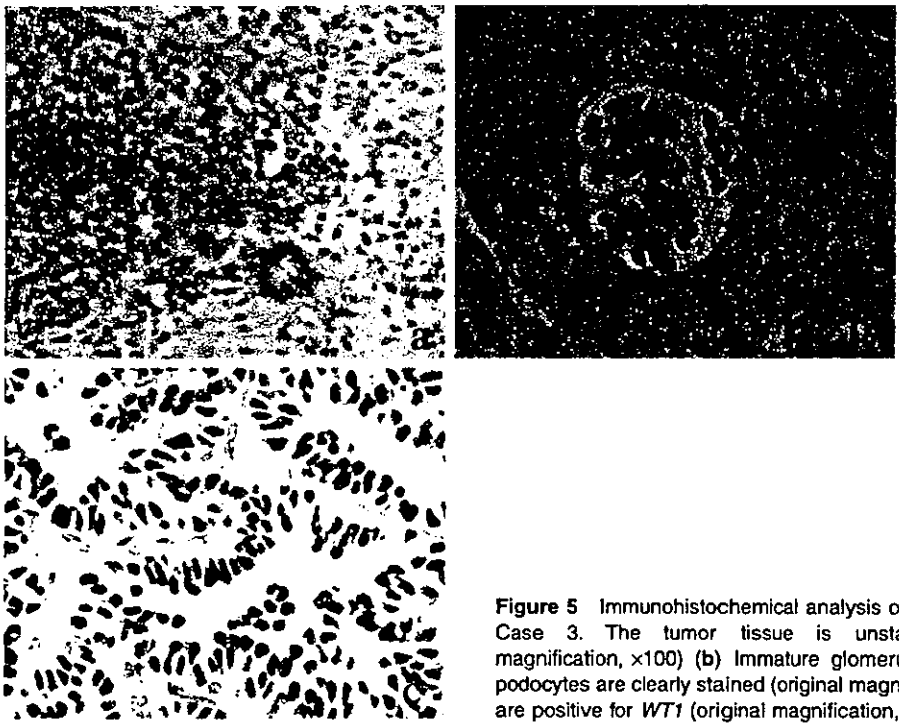

Figure 5 Immunohistochemical analysis of Wilms' tumor suppressor gene (*WT1*). (**a**) Case 3. The tumor tissue is unstained by anti-*WT1* antibody (original magnification, ×100) (**b**) Immature glomerulus in the same section of case 3. The podocytes are clearly stained (original magnification, ×400) (**c**). Case 1. The tumor cells are positive for *WT1* (original magnification, ×400).

proteins with loss of the last zing finger have been previously demonstrated by electrophoretic mobility shift assays.[13] There was a heterozygous mutation at the same point in the germ line of all four patients, thereby supporting the two-hit mutational model of bilateral WT.

In earlier studies, mutation R390X had been found in patients with sporadic unilateral WT, in a patient with bilateral WT, and in a patient with WT associated with urogenital malformation.[14] This mutation has also been detected in a patient with acute promylocytic leukemia[15] and a patient with an isolated genital malformation without WT.[16] Although the histological findings in the WTs with the R390X mutation were not described in the literature, from our results, this R390X mutation might correlate with rhabdomyomatous histology in bilateral WT.

The cases with *WT1* mutation immunohistochemically stained negative for WT1. Loss of *WT1* function has been reported to be the underlying cause of tumor development.[8] Miyagawa *et al.* reported that loss of *WT1* function leads to ectopic myogenesis in WT, and suggested that normal expression of WT1 might prevent the metanephric-mesenchymal stem cells of the kidney from differentiating into skeletal muscle.[17] All four cases had *WT1* mutations, and cases 2 and 4 showed stromal-predominant histology. Cases 3 and 5 showed the nephroblastic type before chemotherapy, and it could not be concluded that all WTs with the R390X mutation present with FRN histologically. Cases 3 and 5 contained skeletal muscle cells as a stromal component. After chemotherapy, case 3 showed FRN and case 5 had more striated muscle cells than before chemotherapy. All

four cases were negative for *WT1*. Loss of *WT1* expression is related to histological features, at least in bilateral WT.

Tumor volume, except for case 1, increased or failed to regress after the usual chemotherapy for classical WT, and the tumors appeared to be resistant to the usual chemotherapy. Histologically, all tumors, except case 1, showed a marked predominance of mature striated muscle, including increased collagen fibers and decreased epithelial and blastemal components, after chemotherapy. Before chemotherapy, all tumor components, stromal, epithelial, and blastemic, were strongly positive for Ki-67, a cell proliferation-related antigen absent in the G0 phase. After chemotherapy,striated muscle, which was the main component of the tumors, was negative for Ki-67. Tubular structures and blastema were positive for Ki-67, but they were a very small component of the tumors. Further, FRN been reported to be a poor responder to preoperative chemotherapy,[4,5] and Anderson *et al.* reported that rhabdomyomatous histology in bilateral Wilms' tumors is associated with poor response to chemotherapy.[18] Except for case 1, tumor volume in either increased or failed to regress after chemotherapy. Histologically, however, the immature component decreased and the mature component increased. The mature component showed less proliferate activity. Apparently, chemotherapy was effective, but tumor volume did not decrease because of the increase in collagen fibers. Most clinicians assume that chemotherapy is ineffective if tumor volume does not change after chemotherapy, and they consider continuous or additional chemotherapy. Additional aggressive chemotherapy consisting of etoposide, carboplatin and cyclophosphamide, which is said to be effective against proliferating tumor cells, was performed in our cases. These anticancer drugs are ineffective against tumors mainly composed of mature striated muscle components. The prognosis of FRN has been said to be good,[3,4] and our four cases have been free of disease since tumor resection. Aggressive chemotherapy, which has little effect on the tumor and might cause complications, should be avoided. The usual chemotherapy for the stage in each side is sufficient. However, there might be residual immature components that show proliferative activity and have the potential to metastasize. Surgical resection of tumors after usual chemotherapy is essential.

Nagashima *et al.* reported myogenic differentiation of stromal cells in the nude mouse WT line.[19] Wilms' tumor tends to spontaneously differentiate into mature elements, although it is not as well known as neuroblastoma. Zuppan *et al.* reported differentiation of WT after preoperative chemotherapy.[20] Seenmayer *et al.* and Ishikawa *et al.* reported a case of WT in which complete maturation of a pulmonary metastasis was documented after chemotherapy.[21,22] Chemotherapy might induce mesenchymal differentiation in WT and promote tumor maturation. The results clearly indicate that immature stromal components in our cases differentiated into mature striated muscles. This maturation is probably attributable to both the inherent nature of WT to differentiate and the effect of chemotherapy.

The histological diagnosis before therapy is important when deciding the management of bilateral WT. If the diagnosis is FRN, chemotherapy could not be expected to result in tumor reduction. Tumors might be resected in the early course of the therapy, for example, after one course of chemotherapy or before chemotherapy, if renal preservation is possible.

In conclusion, the histological features strongly correlate with *WT1* mutation in bilateral WT. Preoperative diagnostic biopsy is important in bilateral WT because if the pathological subtype of the tumor is FRN or it contains striated muscle, tumor volume reduction cannot be the expected response to chemotherapy, even if chemotherapy is effective. Clarification of the biological characteristics of bilateral WT is required in order to determine the most suitable treatment.

ACKNOWLEDGMENTS

We thank Drs H. Horie (Chiba Children's Hospital), K. Hashizume and Y. Kanamori (University of Tokyo Faculty of Medicine), J. Miyauchi and Y. Tsunematsu (National Center for Child Health and Development), Y. Hayashi (Tohoku University School of Medicine) and Y. Ogawa (Saitama Childrenís Medical Center) for providing samples and clinical data. We thank Mr H. Suzuki for his technical assistance.

This work was supported by a Grant-in-Aid for Scientific Research from the Ministry of Education, Culture, Sports, Science and Technology (11557021, 13470053, 13022264 and 11167274), as well as a Cancer Research Grants from the Ministry of Health, Labor and Welfare (9–14, 10D-1).

REFERENCES

1 Coppes MJ, Pritchard-Jones K. Principles of Wilms' tumor biology. *Urol Clin North Am* 2000; **27**: 423–33.
2 Lee SB, Haber DA. Wilms' tumor and the WT1 gene. *Exp Cell Res* 2001; **264**: 74–99.
3 Wigger HJ. Fetal rhabdomyomatous nephroblastoma-a variant of Wilms' tumor. *Hum Pathol* 1976; **7**: 613–23.
4 Maes P, Delemarre J, de Kraker J, Ninane J. Fetal rhabdomyomatous nephroblastoma: a tumour of good prognosis but resistant to chemotherapy. *Eur J Cancer* 1999; **35**: 1356–60.
5 Saba LM, de Camargo B, Gabriel-Arana M. Experience with six children with fetal rhabdomyomatous nephroblastoma: review of the clinical, biologic, and pathologic features. *Med Pediatr Oncol* 1998; **30**: 152–5.
6 Call KM, Glaser T, Ito CY *et al.* Isolation and characterization of a zinc finger polypeptide gene at the human chromosome 11 Wilms' tumor locus. *Cell* 1990; **60**: 509–20.
7 Gessler M, Poustka A, Cavenee W *et al.* Homozygous deletion in Wilms tumours of a zinc-finger gene identified by chromosome jumping. *Nature* 1990; **343**: 774–8.

8 Schumacher V, Schneider S, Figge A *et al.* Correlation of germline mutations and two-hit inactivation of the WT1 gene with Wilms tumors of stromal-predominant histology. *Proc Natl Acad Sci USA* 1997; **94**: 3972–7.
9 Huff V, Miwa H, Haber DA *et al.* Evidence for WT1 as a Wilms tumor (WT) gene: intragenic germinal deletion in bilateral WT. *Am J Hum Genet* 1991; **48**: 997–1003.
10 Knudson AG Jr, Strong LC. Mutation and cancer: a model for Wilms' tumor of the kidney. *J Natl Cancer Inst* 1972; **48**: 313–24.
11 Committee on histological classification of childhood tumors the Japanese pathological society. Histological classification and atlas of tumors in infancy and childhood I T Tumors of the urinary system. In: Urano Y, ed. *Tumors of the Kidneys*. Tokyo: Kanehara, 1988; 12–3.
12 Takata A, Kikuchi H, Fukuzawa R, Ito S, Honda M, Hata J. Constitutional WT1 correlate with clinical features in children with progressive nephropathy. *J Med Genet* 2000; **37**: 698–701.
13 Little M, Holmes G, Bickmore W, van Heyningen V, Hastie N, Wainwright B. DNA binding capacity of the WT1 protein is abolished by Denys–Drash syndrome WT1 point mutations. *Hum Mol Genet* 1995; **4**: 351–8.
14 Little M, Wells C. A clinical overview of WT1 gene mutations. *Hum Mutat* 1997; **9**: 209–25.
15 King-Underwood L, Renshaw J, Pritchard-Jones K. Mutations in the Wilms' tumor gene WT1 in leukemias. *Blood* 1996; **87**: 2171–9.
16 Kohler B, Schumacher V, l'Allemand D, Royer-Pokora B, Grutters A. Germline Wilms tumor suppressor gene (WT1) mutation leading to isolated genital malformation without Wilms tumor or nephropathy. *J Pediatr* 2001; **138**: 421–4.
17 Miyagawa K, Kent J, Moore A *et al.* Loss of WT1 function leads to ectopic myogenesis in Wilms' tumour. *Nat Genet* 1998; **18**: 15–7.
18 Anderson J, Slater O, McHigh K, Duffy P, Pritchard J. Response without shrinkage in bilateral Wilms tumors: Significance of rhabdomyomatous histology. *J Pediatr Hematol Oncol* 2002; **24**: 31–4.
19 Nagashima Y, Nishihira H, Miyagi Y *et al.* A nude mouse Wilms' tumor line (KCMC-WT-1) derived from an aniridia patient with monoalleleic partial deletion of chromosome 11p. *Cancer* 1996; **77**: 799–804.
20 Zuppan CW, Beckwith JB, Weeks DA, Luckey DW, Pringle KC. The effect of preoperative therapy on the histologic features of Wilms' tumor. An analysis of cases from the Third National Wilms' Tumor Study. *Cancer* 1991; **68**: 385–94.
21 Seemayer TA, Harper JL, Shickell D *et al.* Cytodifferentiation of a Wilms' tumor pulmonary metastasis: theoretic and clinical implications. *Cancer* 1997; **79**: 1629–34.
22 Ishikawa K, Toyoda Y, Fukuzato Y, Kato K, Ijiri R, Tanaka Y. Maturation in the primary and metastatic lesions of fetal rhabdomyomatous nephroblastoma. *Med Pediatr Oncol* 2001; **37**: 62–3.

THE JOURNAL OF BIOLOGICAL CHEMISTRY
© 2003 by The American Society for Biochemistry and Molecular Biology, Inc.

Vol. 278, No. 7, Issue of February 14, pp. 5427–5432, 2003
Printed in U.S.A.

Cooperative Interaction of EWS with CREB-binding Protein Selectively Activates Hepatocyte Nuclear Factor 4-mediated Transcription*

Received for publication, October 7, 2002, and in revised form, November 22, 2002
Published, JBC Papers in Press, November 28, 2002, DOI 10.1074/jbc.M210234200

Natsumi Araya‡§, Keiko Hirota‡§, Yoko Shimamoto‡§, Makoto Miyagishi‡§, Eisaku Yoshida§, Junji Ishida‡§, Setsuko Kaneko¶, Michio Kaneko¶, Toshihiro Nakajima‡§, and Akiyoshi Fukamizu‡§**

From the ‡Center for Tsukuba Advanced Research Alliance, Aspect of Functional Genomic Biology, the §Institute of Applied Biochemistry, Tsukuba, Ibaraki 305-8577, and the ¶Department of Pediatric Surgery, Institute of Clinical Medicine, University of Tsukuba, Tsukuba, Ibaraki 305-8575, Japan

The *EWS* gene when fused to transcription factors such as the ETS family *ATF-1*, *Wilms' tumor-1*, and nuclear orphan receptors upon chromosomal translocation is thought to contribute the development of Ewing sarcoma and several malignant tumors. Although EWS is predicted to be an RNA-binding protein, an inherent EWS nuclear function has not yet been elucidated. In this study, we found that EWS associates with a transcriptional co-activator CREB-binding protein (CBP) and the hypophosphorylated RNA polymerase II, which are included preferentially in the transcription preinitiation complex. These interactions suggest the potential involvement of EWS in gene transcription, leading to the hypothesis that EWS may function as a co-activator of CBP-dependent transcription factors. Based on this hypothesis, we investigated the effect of EWS on the activation of nuclear receptors that are activated by CBP. Of nuclear receptors examined, hepatocyte nuclear factor 4-dependent transcription was selectively enhanced by EWS but not by an EWS mutant defective for CBP binding. These results suggest that EWS as a co-activator requires CBP for hepatocyte nuclear factor 4-mediated transcriptional activation.

The *EWS* gene was originally identified in Ewing's sarcoma with the t(11,22) chromosomal translocation where it is fused to the ETS transcription factor *Fli-1* gene (1). Subsequent studies indicated that other ETS transcription factor genes fuse to the *EWS* gene and produce fusion proteins in Ewing's sarcoma. In addition to the fusion with ETS transcription factors in Ewing's sarcoma, the *EWS* gene has been shown to form fusion proteins with ATF-1 in malignant melanoma of soft parts, WT-1 in desmoplastic small round cell tumors, and nuclear orphan receptors in myxoid chondrosarcomas (2). In EWS fusion proteins, the N-terminal domain (NTD)[1] of EWS is retained, whereas the C-terminal domain of EWS is replaced by corresponding fusion partners. However, the roles of EWS in normal cellular functions and the mechanisms whereby EWS fusion proteins lead to these malignant tumors remain unclear.

EWS contains the transcriptional activation domain in its NTD and the RNA-recognition motif and arginine-glycine-glycine repeats (RGG), both of which are found in RNA-binding proteins (3) in its C-terminal domain. Transcriptional and post-transcriptional processing are closely coupled events *in vivo* (4), and based on its structural features, it is likely that EWS participates in RNA transcription and mRNA synthesis. Furthermore, the NTD of EWS associates with the basal transcription factor TFIID (5) and with certain subunits of the RNA polymerase II complex (5, 6). On the other hand, EWS interacts with the splicing factors SF1 (7), U1C (8), TASR-1/TRSR-2 translocation liposarcoma protein-associated serine-arginine protein (9), and Y-box protein-1 (10). A current expectation is that EWS may act as an adaptor molecule linking between gene transcription and mRNA processing by interacting with RNA polymerase II and the splicing factors (2).

Interestingly, in this study, we indicated the interaction of EWS with the transcriptional co-activator CBP and the hypophosphorylated RNA polymerase II. CBP enhances many DNA-binding transcriptional activator proteins including nuclear receptors and other signal-regulated activators by its histone acetyltransferase activity and recruitment of RNA polymerase II-dependent basal transcription complex or other cofactors to target gene promoters (11, 12). Therefore, these identified interactions suggest the potential involvement of EWS in gene transcriptional activation. However, the fact that EWS does not have any significant DNA-binding motifs or binding activity to specific gene promoters prompted us to propose the hypothesis that EWS may function as a co-activator of CBP-dependent DNA-binding transcription factors. Based on this hypothesis, we investigated the possible effects of EWS on transactivation mediated by nuclear receptors. We showed that EWS selectively enhances the nuclear receptor hepatocyte nuclear factor 4 (HNF4)-mediated transcription cooperatively with CBP. These results suggest that EWS not only

* This work was supported in part by Grant JSPS-RFTF 97L00804 from the "Research for the Future" Program (The Japan Society for the Promotion of Science), a grant-in-aid for Scientific Research on Priority Areas and a grant-in-aid for Scientific Research (A) from the Ministry of Education, Science, Sports, and Culture of Japan, and the Research Grant 11C-1 for Cardiovascular Diseases from the Ministry of Health, Labor, and Welfare. The costs of publication of this article were defrayed in part by the payment of page charges. This article must therefore be hereby marked "*advertisement*" in accordance with 18 U.S.C. Section 1734 solely to indicate this fact.

** To whom correspondence should be addressed: Center for Tsukuba Advanced Research Alliance, Institute of Applied Biochemistry, University of Tsukuba, Tsukuba, Ibaraki 305-8577, Japan. Tel./Fax: 81-298-53-6070; E-mail: akif@tara.tsukuba.ac.jp.

[1] The abbreviations used are: NTD, N-terminal domain; Luc, luciferase; tk, thymidine kinase; CREB, cAMP-response element-binding protein; CBP, CREB-binding protein; HNF4, hepatocyte nuclear factor 4; GST, glutathione *S*-transferase; PPAR, peroxisome proliferator-activated receptor; HA, hemagglutinin; GST, glutathione *S*-transferase; G6P, glucose 6-phosphatase; Apo, apolipoprotein; RAR, retinoic acid receptor; Pol, polymerase.

functions as an adaptor molecule for splicing events but also as a co-activator with CBP for transcriptional initiation.

EXPERIMENTAL PROCEDURES

Plasmids—Human EWS deletion mutants were generated by PCR-based subcloning into pGEX5X-1 (Amersham Biosciences) or FLAG-tagged pcDNA3 (Invitrogen). pHNF4x8-tk-Luc and pβREx2-tk-Luc have been described previously (13, 14). pPPREx3-sv-Luc was constructed by ligating the three copies of the peroxisome proliferator-activated receptor (PPARα) binding site encompassing the nucleotide region (−104 to −92) of the 3-hydroxy-3-methyl-glutaryl-CoA synthase to the pGL3-SV40 promoter/luciferase fusion vector (Promega). Apolipoprotein CIII (ApoCIII)-Luc and glucose 6-phosphatase (G6P)-Luc were constructed by PCR-based methods. Human *ApoCIII* promoter (−890 to +44) or human *G6P* promoter (−826 to +3) fragment was inserted into pPicaGene-Basic vector II. Angiotensinogen 13-Luc was constructed by digesting a 1266-bp (−1222 to +44) fragment from human angiotensinogen promoter 13cat, which has been described previously (15), into pPicaGene-Basic vector II (Toyo-ink). pcDNA3-mCBP-HA and pcDNA3-mCBP-FLAG were generated by inserting full-length mouse CBP into HA or FLAG-tagged pcDNA3. pcDNA3-HA-HNF4α was generated by reverse transcription-PCR-based cloning into HA-tagged pcDNA3.

Antibodies—Anti-EWS rabbit polyclonal antibody was generated against a GST-EWS-(246–504). Anti-HNF4 rabbit polyclonal antibody was generated against a GST-HNF4-(133–366). Anti-CBP rabbit polyclonal antiserum-(5614) was described previously (16). Anti-HA monoclonal antibody (12CA5) was purchased from Roche Molecular Biochemicals; anti-FLAG monoclonal antibody (M2) was from Sigma; anti-HNF4α (C-19) and anti-RNA polymerase II (N-20) polyclonal antibodies were from Santa Cruz Biotechnology; and anti-RNA pol II monoclonal antibodies (8WG16 and H14) were from BAbCo.

Cells Culture and Transfections and Reporter Gene Assays—HEK293T cells and HepG2 cells were cultured in Dulbecco's modified Eagle's medium supplemented with 10% fetal bovine serum, and HEK293 cells were maintained in minimum Eagle's medium containing 10% fetal bovine serum. For the reporter gene assay, transfections were performed by the calcium phosphate method. A Rous sarcoma virus-β-galactosidase plasmid was included in each transfection experiment to control for transfection efficiency. The luciferase activity was measured with an ARVO™SX (Wallac Berthold). The values were normalized to β-galactosidase activity as an internal control.

Immunoprecipitation—HEK293T cells were transfected using FuGENE 6 reagents (Roche Molecular Biochemicals), and nuclear extracts were prepared as described previously (13). Nuclear extracts were incubated with anti-FLAG coupled with protein G-agarose in buffer A (20 mM HEPES, pH 7.9, 100 mM NaCl, 1 mM EDTA, 1 mM dithiothreitol, 0.1% Nonidet P-40, 5% glycerol, 1 mM Na_3VO_4, 5 mM NaF, and protease inhibitors) for 4 h at 4 °C. The binding complexes were washed with the same buffer. For co-immunoprecipitation of endogenous EWS, CBP, and HNF4, nuclear extracts of HepG2 cells were subjected to immunoprecipitation with anti-EWS, anti-HNF4, or anti-CBP-(5614) in Co-immunoprecipitation buffer (10 mM HEPES, pH 7.5, 100 mM KCl, 0.1% Nonidet P-40, and protease inhibitors).

GST Pull-down Assay—The GST fusion protein of each EWS mutant was expressed in *Escherichia coli* strain TopXF' (Invitrogen) and purified using glutathione-Sepharose beads (Amersham Biosciences). Protein extracts of HEK293T cells were incubated with each GST fusion protein bound to resin in 1 ml of buffer A for 8 h at 4 °C. After washing the beads with buffer A, bound proteins were fractionated by SDS-PAGE and analyzed Western blotting.

Immunofluorescence—HEK293T or HEK293 cells were plated onto glass coverslips. HEK293T cells were transfected using FuGENE 6 reagents. After 24 h, cells were fixed with 6% paraformaldehyde, permeabilized with 0.1% Triton X-100, and blocked with 1% bovine serum albumin. Cells then were incubated with the primary antibody, mouse anti-FLAG (1:500 dilution), rabbit anti-EWS (1:250 dilution), mouse anti-Pol IIa (1:200 dilution), or mouse anti-Pol IIo (1:100 dilution) antibody followed by staining with Alexa Fluor 488 anti-mouse IgG, Alexa Fluor 488 anti-rabbit IgG, or Alexa Fluor 568 anti-mouse IgG second antibody (1:2000 dilution each; Molecular Probes). Immunofluorescence was analyzed under a confocal microscope (TCS 4D, Leica).

RESULTS

Physical Association of EWS with CBP and RNA Polymerase II—To isolate CBP-interacting proteins, we used a GAL4 DNA-binding domain fused to CBP as a bait in a yeast two-hybrid screening assay (13) in which we identified EWS as a CBP-binding protein. To biochemically characterize the interaction of EWS with CBP, we constructed a series of EWS deletion mutants fused to GST and bacterially expressed products of them for the following assays (Fig. 1*A*). GST pull-down assays were performed on this series of EWS deletions with HEK293T lysates expressing HA-tagged CBP. Western blotting of the bound proteins using anti-HA antibody showed that CBP was specifically retained on beads coupled with GST-EWS-(1–656), GST-EWS-(1–333), and GST-EWS-(83–227) (Fig. 1*B*). These results show that EWS can specifically interact with CBP through its amino acids 83–227 located on the NTD of EWS.

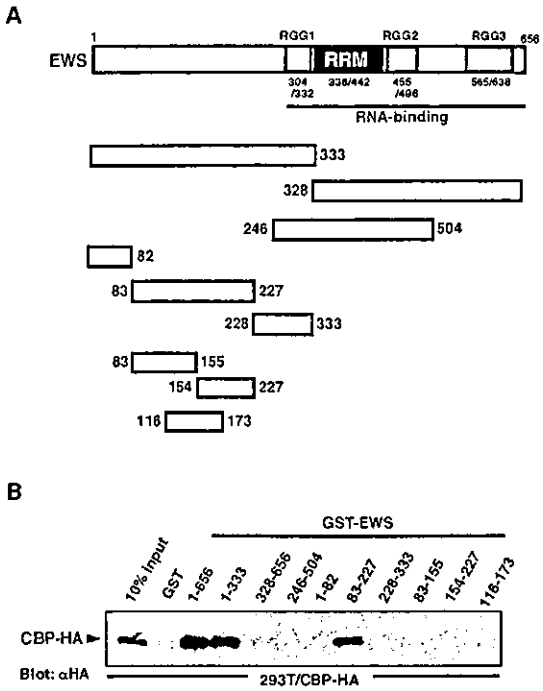

FIG. 1. **Map of the CBP interaction domain in EWS.** *A*, schematic representation of EWS and its deletion mutants in this study. These elements in the C-terminal domain of EWS were commonly found in RNA-binding proteins (3). *B*, *in vitro* binding assay using cell extracts from HEK293T cells transfected with HA-tagged CBP expression plasmid and GST or EWS deletion mutants fused to GST. Western blot analysis was performed with anti-HA antibody (12CA5).

Two isoforms of RNA polymerase II (Pol II) exist *in vivo*, the hypophosphorylated (Pol IIa) and the hyperphosphorylated (Pol IIo) forms required for transcriptional initiation and elongation, respectively. Pol IIa is shown to possess the hypophosphorylated C-terminal domain of the largest subunit and interacts with a range of general transcription factors at the promoter (17, 18). We investigated the relationship of EWS with different forms of Pol II using three anti-Pol II antibodies: N-20, which recognizes the common NTD of both Pol IIa and Pol IIo large subunits; H14, which only recognizes Pol IIo; and 8WG16, which only recognizes Pol IIa in immunofluorescence staining and Western blotting. To test the possible interaction of EWS with distinct forms of Pol II, we first examined their cellular localization. The staining patterns of Pol IIa and Pol IIo were compared with nucleoplasmic EWS distribution in double-labeling experiments followed by a confocal microscopy. The overlay images showed that the nucleoplasmic structures of EWS, and both Pol II forms partially overlapped (Fig. 2*A*). To further confirm the biochemical interaction of EWS with both Pol IIa and Pol IIo, we performed GST pull-down assays using HEK293 nuclear extracts. GST-EWS combined with both Pol IIa and Pol IIo *in vitro*, whereas GST alone did not (Fig. 2*B*). As shown in Fig. 2*C*, both EWS and CBP associated with the

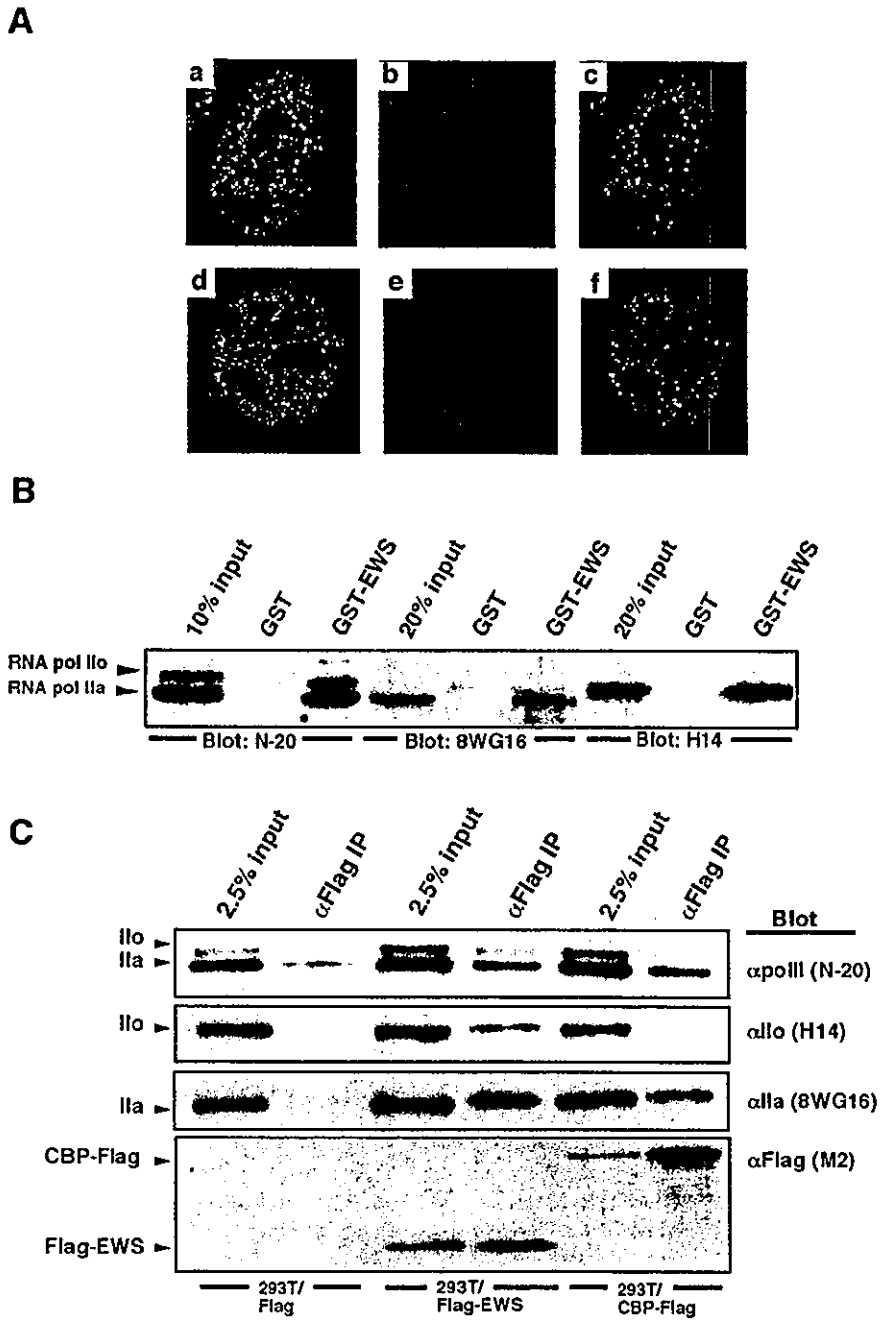

FIG. 2. ***In vitro* and *in vivo* association of EWS with Pol II.** *A*, co-localization of endogenous EWS and Pol IIa or Pol IIo by immunofluorescence staining. Fixed HEK293 cells were double-labeled with anti-EWS antibody (*panels a* and *d*) and 8WG16 against Pol IIa (*panel b*) or H14 against Pol IIo (*panel e*), whereas coincident signals are seen in *yellow* in the overlay pictures obtained by a confocal microscopy (*panel c* and *f*). *B*, interaction of EWS with Pol II *in vitro*. Nuclear extracts from HEK293 cells were incubated with GST or GST-EWS-(1–656). Bound Pol II was visualized by Western blot analysis using anti-Pol II antibodies N-20, 8WG16, or H-14. *C*, co-immunoprecipitation of Pol II using FLAG-tagged EWS or CBP. Nuclear extracts from HEK293T cells transfected with FLAG-tagged EWS, or CBP expression plasmids were immunoprecipitated with anti-FLAG antibody (M2) and subjected to immunoblotting with anti-Pol II (N-20, 8WG16, or H14) or anti-FLAG (M2) antibodies.

preinitiation form of Pol II (pol IIa), whereas EWS but not CBP co-immunoprecipitated with Pol IIo *in vivo*. These results suggest that EWS is spatially and physically included in a part of both of the preinitiation and elongation Pol II complexes.

Selective Enhancement of HNF4-mediated Transactivation by EWS—To examine the potential role of EWS in nuclear receptors-mediated transactivation, we evaluated the effects of EWS on the activation of three nuclear receptors including HNF4, retinoic acid receptor (RAR), and PPARα by transfection experiments. A role for EWS as a co-activator in HNF4-mediated transactivation was first tested using HNF4-specific reporter, pHNF4x8-tk-Luc (13). As shown in Fig. 3*A*, transfection of HEK293 cells with the reporter alone or with HNF4 resulted in activation (Fig. 3*A1*), which was stimulated 5-fold by co-transfection of EWS (Fig. 3*A*, *1* and *2*). We also examined the effect of EWS on RAR-mediated transactivation using RAR-specific reporter, pβREx2-tk-Luc (14). HEK293 cells express the endogenous RAR as the reporter activity was sufficiently activated by its cognate ligand, even without co-transfection of RAR expression plasmids (Fig. 3*B1*). Co-transfection of EWS repressed this activity by an RAR-specific ligand (Fig. 3*B*, *1* and *2*). Similar experiments were carried out using PPARα with pPPREx3-sv-Luc. As shown Fig. 3*C*, no effect of EWS was found on the activity of this receptor. Taken together, these results suggest that EWS is a selective co-activator for HNF4-mediated transactivation.

Formation of EWS, CBP, and HNF4 complex and Cooperative Enhancement of HNF4-dependent Transactivation—HNF4, which belongs to nuclear receptor superfamily, is a liver-enriched DNA-binding transcription factor. Binding sites for HNF4 have often been found in the regulatory regions of a large number of genes involved in fatty acid metabolism (19), gluconeogenesis (20), and blood pressure control (15) and in determining the hepatic phenotype (21). To test for transcriptional co-activations by EWS on the endogenous promoter sequences, we carried out transfection experiments using lucif-